Tetrahedron 68 (2012) 3626–3632

Contents lists available at SciVerse ScienceDirect

Tetrahedron

journal homepage: www.elsevier.com/locate/tet

Y-shaped dyes based on triphenylamine for efficient dye-sensitized solar cells

Junhui Jia [a], Kaiyu Cao [a], Pengchong Xue [a,*], Yuan Zhang [b], Huipeng Zhou [a], Ran Lu [a,*]

[a] State Key Laboratory of Supramolecular Structure and Materials, College of Chemistry, Jilin University, Changchun 130012, PR China
[b] College of Chemistry, Beijing Normal University, Beijing 100875, PR China

ARTICLE INFO

Article history:
Received 7 November 2011
Received in revised form 15 February 2012
Accepted 28 February 2012
Available online 13 March 2012

Keywords:
Dye-sensitized solar cells (DSSCs)
Triphenylamine
Y-shaped conformation
Carbazole
Phenothiazine

ABSTRACT

Three new triphenylamine-based dyes with Y-shaped conformation bearing triphenylamino-vinyl, 10-octyl-10*H*-phenothiazine-vinyl and 9-octyl-9*H*-carbazole-vinyl as arms (**TT**, **TP**, and **TC**) have been synthesized. From electrochemical investigations it is found that they can be employed in DSSCs due to the balanced HOMO and LUMO energy levels. Notably, the photo-to-electrical conversion efficiency of the DSSCs sensitized with branched **TT**, **TP**, and **TC** reach 5.12%, 4.84%, and 3.63%, which are higher than that sensitized with **T** (2.79%), and the DSSC sensitized with **TT** shows higher IPCE response and better photovoltaic performances (J_{sc}=12.37 mA/cm^2, V_{oc}=0.72 V and ff=0.58) than others. These results reveal that the introduction of branched Y-shaped extended π-conjugated donors to D-π-A dyes cannot only enlarge the spectral response range, but also suppress the molecular aggregation on TiO_2 films to a certain extent, which would enhance the performance of DSSCs.

1. Introduction

Sustained increase in energy demands and concerns about global warming have led to a greater focus on renewable energy sources. It is well-known that solar energy is the largest renewable carbon-free resource. Among the devices that can convert solar energy into electricity, dye-sensitized solar cells (DSSCs) have gained widespread interest due to their high-energy conversion efficiency and low production cost.[1] Although the high power conversion efficiencies above 11% under standard solar illumination have been reported using Ru(II) polypyridyl complexes as the sensitizers in DSSCs,[2] the limited resources and elaborated purification of Ru complexes make the wide application become difficult. In recent years, metal-free organic sensitizers have emerged as competitive alternatives because of relatively low cost, ease of structural tuning, high molar extinction coefficients, and more environmentally friendly properties.[3] Although the energy conversion efficiencies of the DSSCs sensitized with organic dyes have been improved greatly,[4] the conversion efficiencies still lag behind those of the Ru complexes. It is suggested that the narrow absorption bands in the visible region and the formation of aggregates on the semiconductor surfaces are responsible for the low efficiencies of organic dyes compared to the ruthenium sensitizers.[5] Therefore, on the one hand, many attempts have been made to design organic dye molecules with higher molar extinction coefficients and broader spectral responses, and it is found that most of the efficient organic dyes synchronously contain donor and acceptor bridged by a π-conjugated linker (D-π-A) because their spectral responses can be tuned by varying donor, spacer, and acceptor moieties. For example, the derivatives of porphyrin,[4i] thiophene,[4m,n] fluorene,[4k] phenothiazine,[4p,q] carbazole,[4f,r] coumarin,[4s] indoline,[4g] cyanine,[4t] hemicyanine,[4u] merocyanine,[4v] perylene,[4w] and triarylamine,[4a,j,6–8] used as the sensitizers have yielded good conversion efficiencies. On the other hand, in order to avoid molecular aggregation of the organic dyes starburst units were employed in the conjugated molecules.[4h,n,9] With these in mind, we designed new branched triphenylamine-based conjugated molecules in Y-shaped conformation, in which two arms of triphenylamino-vinyl, 10-octyl-10*H*-phenothiazine-vinyl or 9-octyl-9*H*-carbazole-vinyl were anchored by a triphenylamine moiety connected with the acceptor of cyanoacrylic acid (**TT**, **TP**, and **TC**, Scheme 1). Such extended π-conjugated systems with branched arms are expected to exhibit strong light-harvesting abilities and weak aggregation tendency. It has been found that the total solar-to-energy conversion efficiencies of the devices sensitized with Y-shaped **TT**, **TP**, and **TC** are 5.12%, 4.84%, and 3.63%, respectively, which are higher than that of the device sensitized with **T** (2.79%). It suggests that the introduction of the branched Y-shaped donor with extended π-conjugation to D-π-A dyes would enhance the performance of the DSSCs.

---

* Corresponding authors. Tel.: +86 431 88499179; e-mail addresses: xuepengchong@mail.jlu.edu.cn (P. Xue), luran@mail.jlu.edu.cn (R. Lu).

0040-4020/$ – see front matter © 2012 Elsevier Ltd. All rights reserved.
doi:10.1016/j.tet.2012.02.077

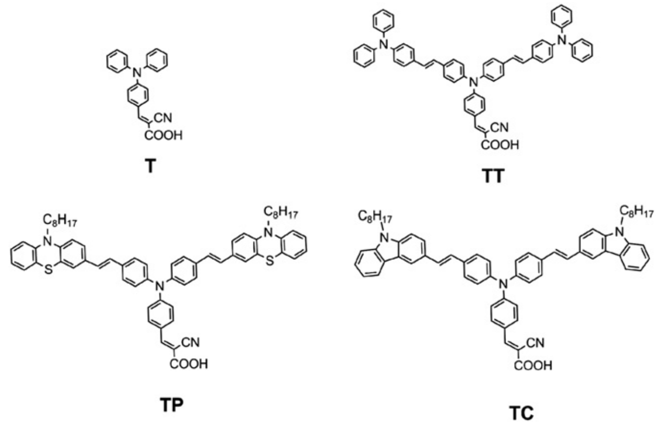

Scheme 1. Molecular structures of triphenylamine-based dyes **T**, **TT**, **TP**, and **TC**.

2. Results and discussion

2.1. Syntheses of TT, TP, and TC

The synthetic routes for triphenylamine-based dyes **TT**, **TP**, and **TC** are sketched in Scheme 2. Compounds **1**–**3** were synthesized according to the reported procedures.[10,11] The Heck reaction between compounds **1** and **2** catalyzed by $Pd(OAc)_2$ at 110 °C for 24 h afforded compound **5** in a yield of 78%.[10] Then, compound **5** could be easily transformed into compound **TT** via Knoevenagel reaction in a yield of 74%.[6] Similarly, compound **TP** was prepared from compound **6**, which was obtained from compounds **1** and **3** under Heck reaction condition. Moreover, Wittig reaction between methyltriphenylphosphonium iodine and 9-octyl-9*H*-carbazole-3-carbaldehyde[12] gave compound **4**, which reacted with compound **1** via Heck reaction to yield compound **7**. Thus, compound **TC** was synthesized by Knoevenagel reaction between cyanoacetic acid and compound **7** in a yield of 68%. In addition, we synthesized 3-(4-diphenylaminophenyl)-2-cyanoacrylic acid (**T**) as the reference compound according to the reported procedures.[7] All the intermediates and the target products were purified by column chromatography, and the new compounds were characterized with FTIR, ^{1}H NMR, ^{13}C NMR, elemental analysis, and MALDI/TOF mass spectroscopy. The compounds **TT**, **TP**, and **TC** exhibited vibration absorption bands around 962 cm^{-1} in the IR spectrum, suggesting the presence of the trans-double bond (C=C).[6,11] In addition, the ^{1}H NMR spectra of **TT**, **TP**, and **TC** further confirmed that all the ethenyl groups adopted the trans-conformation on account of the absence of the signal at ~6.5 ppm assigned to the protons in cis-double bonds (CH=CH).[6,11,13] The obtained dyes **TT**, **TP**, and **TC** showed good solubility in most organic solvents, including toluene, benzene, *o*-dichlorobenzene, CH_2Cl_2, THF, $CHCl_3$, DMF, DMSO, etc.

2.2. Photophysical properties

As shown in Fig. 1a, it was found that the π–π^* transition absorption band of **T** in THF (2.0×10^{-5} M) appeared at 300 nm, and its intermolecular charge transfer (ICT) transition band emerged at 370 nm. As to **TT**, **TP**, and **TC**, the absorption bands originated from ICT transition red-shifted to 407, 409, and 395 nm (Table 1), respectively, compared with that of **T**. Such spectral changes may be due to the extended π-conjugation of the branched Y-shaped triphenylamines. In addition, the molar extinction coefficients of **TT** (6.67×10^4 M^{-1} cm^{-1} at 407 nm), **TP** (5.40×10^4 M^{-1} cm^{-1} at 409 nm) and **TC** (4.74×10^4 M^{-1} cm^{-1} at 395 nm) were higher than that of **T** (0.94×10^4 M^{-1} cm^{-1} at 370 nm, Table 1) meaning that the stronger light-harvesting abilities of the triphenylamine-based dyes than that of **T** could be expected. Moreover, the UV–vis absorption spectra of triphenylamine-based dyes deposited on transparent TiO_2 films (2 μm in thickness) were shown in Fig. 1b. The maximal absorption peaks for **T**, **TT**, **TP** and **TC** on TiO_2 films appeared at 387, 408, 444 and 428 nm, respectively, exhibiting red-shift compared with those in solutions, which might originate from the aggregation or electronic coupling of dyes on the TiO_2 surfaces.[14] It should be noted that there is a red-shift of 1 nm for **TT** on TiO_2 film compared with that in solution was detected, meaning that the branched conformation of **TT** could suppress the formation of the aggregates effectively on TiO_2 surface. Furthermore, the

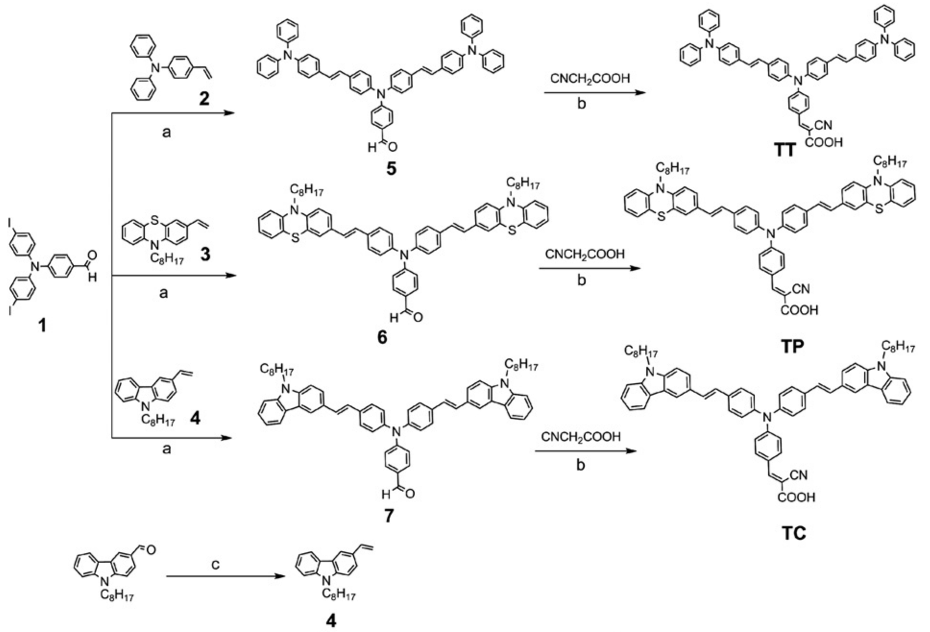

a. $Pd(OAc)_2$, K_2CO_3, TBAB, dry DMF, 110°C, N_2, 24h; b. NH_4OAc, CH_3COOH, 120°C, 12 h

c. dry THF, t-BuOK, $[Ph_3PCH_3]^+I^-$, 0°C~r.t.

Scheme 2. Syntheses of triphenylamine-based dyes **TT**, **TP**, and **TC**.

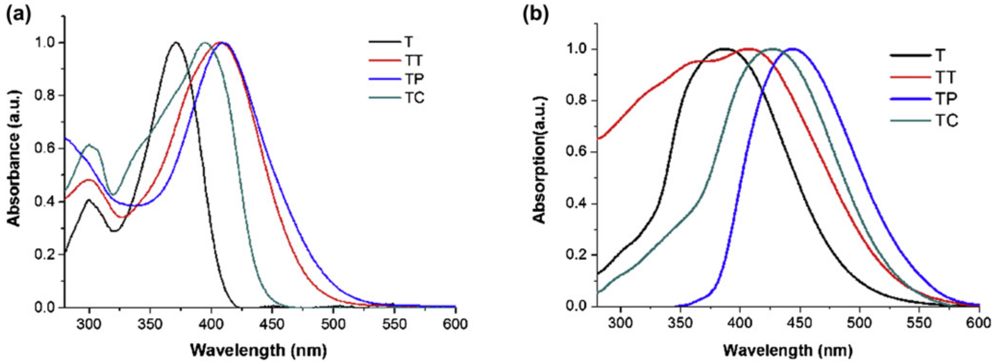

Fig. 1. Normalized UV–vis absorption spectra of triphenylamine-based dyes **T**, **TT**, **TP**, and **TC** in THF (a, 2.0×10^{-5} M) and deposited on TiO_2 films (b).

Table 1
Photophysical and electrochemical data of dyes **T**, **TT**, **TP**, and **TC**

Dye	λ_{abs} (nm) ($\varepsilon\times10^{-4}$ M^{-1} cm^{-1})[a]	E_{ox} (V) versus NHE[b]	E_{0-0} (eV)[c]	E_{LUMO} (V) versus NHE[d]	E_{gap}[e] (V)	HOMO[f] (eV)	LUMO[f] (eV)
T	300 (0.15) 370 (0.94)	0.98	2.49	−1.51	1.01	−5.45	−2.25
TT	300 (3.26) 407 (6.67)	0.47	2.29	−1.82	1.32	−4.80	−2.33
TP	281 (3.45) 409 (5.40)	0.57	2.34	−1.77	1.27	−4.88	−2.36
TC	300 (2.82) 395 (4.74)	0.64	2.28	−1.64	1.14	−4.85	−2.28

[a] Measured in THF (2×10^{-6} M), ε ($\times10^{-4}$ M^{-1} cm^{-1}).
[b] The ground station potential (first oxidation peak) of the dyes was measured in CH_2Cl_2 with ferrocene/ferrocenium (Fc/Fc^+) as an internal reference.
[c] E_{0-0} was determined from the edge of the absorption spectrum without adding TBAOH.
[d] $E_{LUMO}=E_{ox}-E_{0-0}$.
[e] E_{gap} is the energy gap between the E_{LUMO} of the dye and the conduction band level of TiO_2 (−0.5 eV vs NHE).
[f] Energy levels of HOMO and LUMO versus vacuum were given after geometrical optimization.

absorption band of **TT** on TiO_2 film became very broader compared with those of **T**, **TP** and **TC** since the former one might originate from the overlap of the electronic transition bands of **TT** from a large amount of monomeric species and parts of aggregated species, and the later ones mainly from the aggregated species of **T**, **TP** and **TC**. Therefore, the strong light-harvesting ability of **TT** with less aggregation on TiO_2 film would be favoring the performance of DSSC.[4p] In addition, the amount of dyes adsorbed on TiO_2 films was estimated by desorbing the dye with NaOH solution (Table 2).[6,7]

Table 2
Photovoltaic parameters of the DSSCs sensitized with **T**, **TT**, **TP**, and **TC** in full sunlight (AM 1.5 G, 100 mW/cm^2)

Dye	Dye load[a] (10^{-7} mol/cm^2)	V_{oc} (V)	J_{sc} (mA/cm^2)	ff	η (%)
T	1.68	0.64	6.88	0.63	2.79
TT	2.01	0.72	12.37	0.58	5.12
TP	2.08	0.74	11.11	0.59	4.84
TC	1.80	0.73	9.42	0.53	3.63

[a] Amount of the dyes absorbed on TiO_2 film.

2.3. Electrochemical properties

To estimate the HOMO levels of the dyes, cyclic voltammetry was employed using a three-electrode cell and an electrochemistry workstation (CHI 604). The working electrode was a glass carbon disc, the auxiliary electrode was a Pt wire, and Ag/Ag^+ was used as reference electrode. Tetrabutylammonium tetrafluoroborate ($TBABF_4$, 0.1 M) was used as the supporting electrolyte in dry CH_2Cl_2 and the ferrocenium/ferrocene (Fc/Fc^+) redox couple was used as an internal potential reference.[15] It was found that the first oxidation potentials (E_{ox}), corresponding to the HOMO levels, for **TT**, **TP**, and **TC** were 0.47 V, 0.57 V, and 0.64 V (vs NHE, Table 1), respectively, which were more positive than the iodine/iodide redox potential value (0.4 V vs NHE, Fig. 3), so the oxidized dyes formed after electron injection into the conduction band of TiO_2 would accept electrons from I^- thermodynamically.

In addition, the excited-state oxidation potential of the dye plays an important role in the electron-injection process from the excited-state dye to TiO_2 electrode, and it can be evaluated from the equation: $E_{LUMO}=E_{ox}-E_{0-0}$, in which E_{ox} is the first oxidation potentials and E_{0-0} is the 0–0 excitation energy. We gained the E_{0-0} values of **T**, **TT**, **TP**, and **TC** from the edge of absorption spectra of the dyes in dichloromethane, which were 2.49 V, 2.29 V, 2.34 V, and 2.28 V, respectively. As a result, E_{LUMO} values for **T**, **TT**, **TP**, and **TC** were −1.51 V, −1.82 V, −1.77 V, and −1.64 V versus NHE, respectively. The excited-state oxidation potentials of the three Y-shaped triphenylamine-based dyes are more negative than the equivalent potential of the TiO_2 conduction band edge (−0.5 V vs NHE),[1] providing thermodynamic driving force (1.14–1.32 V, Table 1) for electron injection. Therefore, the obtained sensitizers might be employed in DSSCs as sensitizers based on the assumption that energy gap of 0.2 eV is necessary for efficient electron injection.[7,15–17]

2.4. Molecular orbital calculations

To gain an insight into the geometrical and electronic structures of the dyes, density functional theory (DFT) calculations for the four triphenylamine-based sensitizers were performed. Fig. 2 showed the molecular frontier orbitals of **T**, **TT**, **TP**, and **TC**. We could find that the HOMOs of **TT**, **TP**, and **TC** were mainly localized on the donors of triphenylamino-vinyl, 10-octyl-10*H*-phenothiazine-vinyl, and 9-octyl-9*H*-carbazole-vinyl arms, while the HOMO of **T** was a π-orbital delocalized throughout the entire molecule. On the other hand, the LUMOs of **TT** and **TP** were chiefly localized at cyanoacrylic acid groups. It suggested that the modifying of the donor moieties in triphenylamine functionalized cyanoacrylic acid with

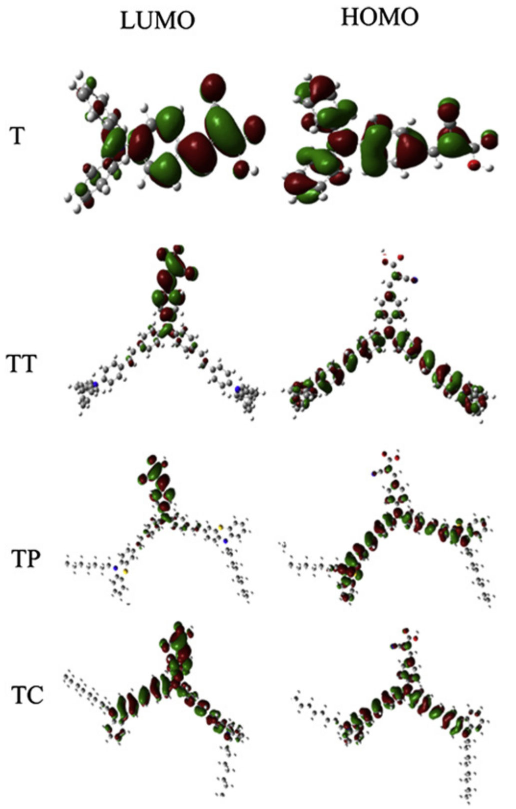

Fig. 2. The frontier orbital plots of the HOMO and LUMO of **T**, **TT**, **TP** and **TC**.

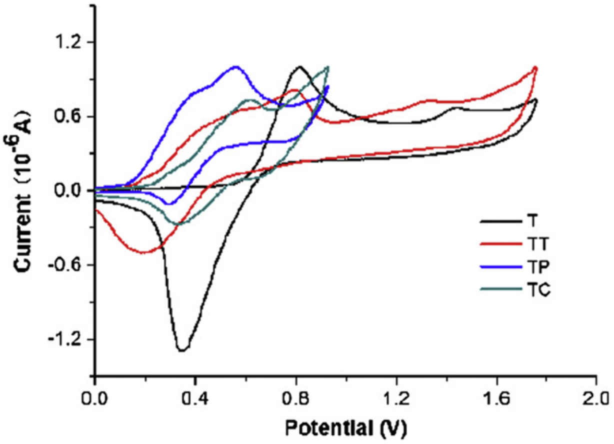

Fig. 3. Cyclic voltammograms of **T**, **TT**, **TP**, and **TC**.

triphenylamine or 10-octyl-10*H*-phenothiazine could lead to a better electron separation between the HOMO and LUMO, which would suppress the electron recombination from the conduction of TiO_2 to the oxidized dyes. However, the LUMO for **TC** was localized not only on cyanoacrylic acid group but also on the carbazole-based arms, which would be unfavorable for the conversion efficiency of the cell, which was confirmed by the following results.

2.5. Photovoltaic properties of DSSCs

The electrochemical cell used for photovoltaic measurements consisted of a dye-adsorbed TiO_2 electrode (the thickness of TiO_2 film is 7 μm), a counter electrode, and an organic electrolyte. The dye-adsorbed TiO_2 electrode and Pt-counter electrode were assembled into a sealed sandwich type cell. The photocurrent–voltage curves of the devices were shown in Fig. 4. The photovoltaic parameters, such as conversion efficiency (η), short-circuit photocurrent density (J_{sc}), the open-circuit photovoltage (V_{oc}), and the fill factor (ff) of the devices under full sunlight (AM 1.5 G, 100 mW/cm^2) were summarized in Table 2. Under standard global AM 1.5 solar conditions, the power conversion efficiencies (η) of the cells sensitized with **TC**, **TP**, and **TT** were 3.63%, 4.84%, and 5.12%, respectively, which were higher than that sensitized with **T** (2.79%), illustrating that the introduction of branched conjugated arms would improve the conversion efficiencies of the DSSCs. As reported by other groups, the DSSCs sensitized with triphenylamine-based dyes have shown the power conversion efficiencies in the range of 3.5–5.8%,[4o,7,8] so the synthesis of the branched triphenylamine-based dyes would be helpful for design of the sensitizers employed in DSSCs. In addition, the J_{sc} and V_{oc} values for the devices based on **TT**, **TP**, and **TC** were also increased compared with that based on **T**. The increased J_{sc} value suggested high extinction coefficient of the Y-shaped dyes,[9] and the increased V_{oc} values of **TT** (0.72 V), **TP** (0.74 V), and **TC** (0.73 V) compared with **T** (0.64 V) could be attributed to the effective retardation of charge recombination between the electrons at the TiO_2 and the oxidized branched dyes.[18,19] To reveal the origin of the increased V_{oc} value for the cells based on **TT**, **TP**, and **TC**, the dark *I*–*V* curves were given in Fig. 3. The onsets of the dark current of the DSSCs based on **TT**, **TP**, and **TC** were 769 mV, 770 mV, and 796 mV, respectively, were higher than **T**-based cell (660 mV), indicating that the increasing of V_{oc} was associated with the decreasing of the electron recombination in TiO_2 with the I^-/I_3^- redox couple in the electrolyte.[20] Notably, we could find that the **TT**-sensitized cell exhibited better photovoltaic performances (J_{sc}=12.37 mA/cm^2, V_{oc}=0.72 V, ff=0.58, and η=5.12%) than other dyes, which might be due to the weakest aggregation of **TT** on TiO_2 film according to UV–vis absorption results. Moreover, the best IPCE (monochromatic incident photon-to-current conversion efficiency) response of **TT**-based DSSC among the obtained DSSCs was also observed as shown in Fig. 5. It was found that the characteristics of the spectral response of the photocurrent for the cells based on triphenylamine-based dyes were similar to their absorption spectra, but the spectral response of the device sensitized by **TT**, **TP**, and **TC** was broader than that of **T** due to their large conjugation. It should be noted that the IPCE curve of the device sensitized with **TT** showed a high plateau from 420 to 520 nm, with maximum of 73% at 423 nm, which was higher than the DSSCs sensitized with other dyes. We deduced that the high IPCE response of the DSSC based on **TT** is probably due to its high

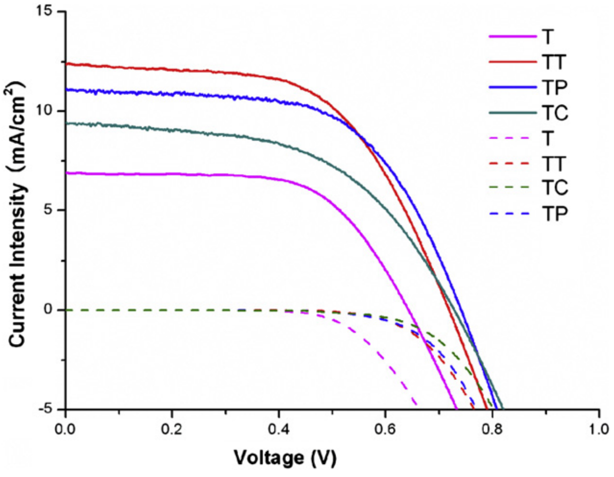

Fig. 4. Current density–voltage curves under full sunlight (real) (AM 1.5 G, 100 mW/cm^2) and in the dark (dashed) of devices sensitized with **T**, **TT**, **TP**, and **TC** using a volatile electrolyte.

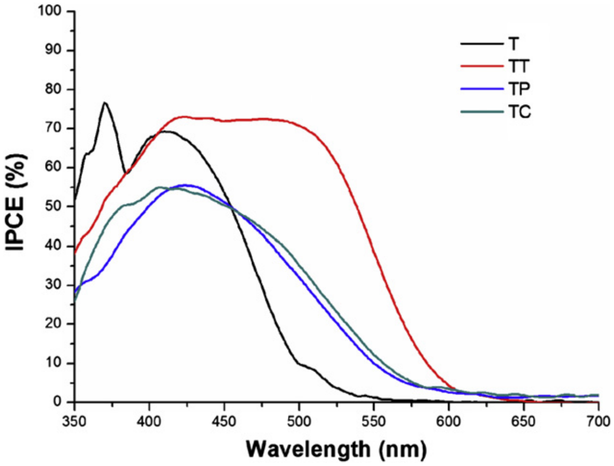

Fig. 5. Incident photo-to-current conversion efficiency of devices sensitized with **T**, **TT**, **TP**, and **TC**.

molar extinction coefficient as well as large energy gap between the LUMO level of the dye and the conduction band edge of TiO_2, which leads to increased electron injection efficiency relative to those of **T**, **TP**, and **TC**.[7,15] Moreover, the branched features (Fig. S2) of the synthesized triphenylamine derivatives would passivate the dyes by blocking the acceptor species from being attracted to the dye molecules.[21] Long-term stability measurements of the devices with quasi-solid-state electrolyte were performed over 720 h at full sunlight and at 50 °C. The variations of the conversion efficiency of solar cells sensitized with **T**, **TT**, **TP**, and **TC** were shown in Fig. S1. As for the full sunlight soaking test, all the four cells show an increase η during the initial 60 h, which may be caused by filling of electrolyte into the inner mesopores of TiO_2 electrode. On continuous 720 h of sunlight soaking test, the solar cell performances of the DSSCs based on the new Y-shaped triphenylamine-based dyes (**TT**, **TP**, and **TC**) show little degradation (3%, 4%, and 7%, respectively), while **T** decreased sharply (18%). Therefore, the stability of **TT** and **TP** under sunlight and air was good.[14] As a result, Y-shaped triphenylamine-based dyes can become competitive candidate in sensitizers employed in DSSCs with high performance on account of their strong light-harvesting ability (extended π-conjugation), weak aggregation (branched structure) on TiO_2 films, and balanced oxidation–reduction potential.

3. Conclusions

In summary, we have synthesized three new Y-shaped triphenylamine-based dyes (**TT**, **TP**, and **TC**), which can be used as sensitizers in DSSCs. It was found that the photo-to-electrical conversion efficiency of the DSSCs sensitized with branched **TT**, **TP**, and **TC** were 5.12%, 4.84%, and 3.63%, which were higher than that sensitized with **T** (2.79%). Notably, the DSSC sensitized with **TT** gave higher IPCE response and better photovoltaic performances (J_{sc}=12.37 mA/cm^2, V_{oc}=0.72 V, and ff=0.58) than others. Therefore, the branched Y-shaped triphenylamine-based dyes with extended π-conjugation could afford high performance of DSSCs on account of their strong light-harvesting ability, weak aggregation on TiO_2 films, and balanced oxidation–reduction potential. This strategy would be helpful for the design of competitive dyes employed in DSSCs.

4. Experimental section

4.1. Materials and measurements

UV–vis absorption spectra were determined on a Shimadzu UV-1601PC spectrophotometer. Photoluminescence (PL) spectra were carried out on a Shimadzu RF-5301 luminescence spectrometer. IR spectra were measured using a Germany Bruker Vertex 80v FT-IR spectrometer by incorporating samples in KBr disks. Mass spectra were performed on Agilent 1100 MS series and AXIMA CFR MALDI/TOF (matrix assisted laser desorption ionization/time-of-flight) MS (COMPACT). C, H, and N analyses were taken on a Vario EL cube elemental analyzer. Cyclic voltammetry was carried out with a CHI 604B electrochemical working station at room temperature at a scan rate of 50 mV/s. Tetrahydrofuran (THF) was distilled over sodium and benzophenone. CH_3CN and DMF were distilled from phosphorous pentoxide. CH_2Cl_2 was distilled by hydrogenated calcium and other chemicals were used as received without further purification. FTO glasses (2.2 mm thickness, 15 Ω/cm^2, Nippon Sheet Glass) pasted with nanocrystalline-TiO_2 in thickness of 7 µm and Pt electrodes were bought from Dalian HeptaChroma SolarTech Co., Ltd.

4.2. Synthetic methods and characterizations

*4.2.1. Compounds **1**–**3**.* Compounds **1** (4-(bis(4-iodophenyl)amino) benzaldehyde), **2** (*N*,*N*-diphenyl-4-vinylaniline), **3** (10-octyl-3-vinyl-10*H*-phenothiazine) and **T** (2-cyano-3-(4-(diphenylamino) phenyl)acrylic acid) were synthesized according to the reported procedures.[7,10,11]

*4.2.2. 9-Octyl-3-vinyl-9H-carbazole (**4**).* Methyltriphenylphosphonium iodine (7.90 g, 19.5 mmol), compound **1** (4.00 g, 13 mmol), and *t*-BuOK (2.30 g, 20 mmol) were dissolved in 25 ml dry THF at 0 °C, and the solution was stirred at room temperature for 3 h. After filtrated to remove the solid, the solvent was removed under reduced pressure. The residue was purified using column chromatography (petroleum ether/CH_2Cl_2=4:1) to give green-yellow oil (3.2 g, 80% in yield). ^{1}H NMR (500 MHz, $CDCl_3$) δ=8.05 (t, *J*=8.5 Hz, 2H), 7.51 (d, *J*=8.5 Hz, 1H), 7.39 (t, *J*=7.5 Hz, 1H), 7.31 (d, *J*=8.0 Hz, 1H), 7.25 (d, *J*=8.5 Hz, 1H), 7.17 (t, *J*=7.5 Hz, 1H), 6.86 (m, 1H), 5.73 (d, *J*=17.5 Hz, 1H), 5.14 (t, *J*=14 Hz, 1H), 4.15 (t, *J*=7.5 Hz, 2H), 1.18–1.26 (m, 12H), 0.84 (t, *J*=7.0 Hz, 3H) (Fig. S3). Anal. Calcd (%) for $C_{22}H_{27}N$: C, 86.51; H, 8.91; N, 4.59. Found: C, 86.39; H, 8.83; N, 4.74.

*4.2.3. 4-(Bis-(4-(4-diphenylaminostyryl)phenyl)-amino)benzaldehyde (**5**).* To a solution of compound **1** (5.25 g, 10 mmol), compound **2** (7.0 g, 26 mmol) and Bu_4NBr (9.85 g, 30 mmol) in dry DMF (50 mL), anhydrous K_2CO_3 (4.2 g, 30 mmol), and $Pd(OAc)_2$ (5.0 mg, 0.02 mmol) were added. The mixture was stirred under a N_2 atmosphere at 110 °C for 24 h. After cooling to room temperature, the mixture was poured into water (500 mL) and extracted with CH_2Cl_2. The combined organic phases were washed with brine, and dried with anhydrous Na_2SO_4. After the solvent was removed, the residue was purified by column chromatography (silica gel, petroleum ether/CH_2Cl_2=2:1) to give 6.3 g yellow solid (78% in yield). Mp 160.0–162.0 °C. ^{1}H NMR (500 MHz, $CDCl_3$) δ=9.83 (s, 1H), 7.71 (d, *J*=8.5 Hz, 2H), 7.45 (d, *J*=8.5 Hz, 4H), 7.38 (d, *J*=8.5 Hz, 4H), 7.27 (m, 8H), 7.13 (m, 12H), 7.03 (m, 12H), 6.96 (d, *J*=16.5 Hz, 2H) (Fig. S4). MS (MALDI-TOF): *m*/*z* 811.9 [M$^+$] (Fig. S5, calcd for $C_{59}H_{45}N_3O$ 811.4). Anal. Calcd (%) for $C_{59}H_{45}N_3O$: C, 87.27; H, 5.59; N, 5.17; O, 1.97. Found: C, 87.15; H, 5.79; N, 5.37.

*4.2.4. 4-(Bis-4-(E-2-(10-octyl-10H-phenothiazin-2-yl)vinyl)phenyl) aminobenzaldehyde (**6**).* The synthetic method for compound **6** was similar to that of compound **5**. It was purified by column chromatography (silica gel, petroleum ether/CH_2Cl_2=4/1) to give yellow solid (60% in yield). Mp 65.0–66.0 °C. ^{1}H NMR (500 MHz, $CDCl_3$) δ=9.83 (s, 1H), 7.70 (d, *J*=8.5 Hz, 2H), 7.42 (d, *J*=8.0 Hz, 4H), 7.27 (d, *J*=17.0 Hz, 4H), 7.13 (d, *J*=8.5 Hz, 8H), 7.09 (d, *J*=8.5 Hz, 2H), 6.90 (d, *J*=33.5 Hz, 10H), 3.75 (t, *J*=6.5 Hz, 4H), 1.25–1.44 (m, 24H), 0.86 (t, *J*=6.5 Hz, 6H) (Fig. S6). MS (MALDI-TOF): *m*/*z* 944.4 [M+H$^+$] (Fig. S7, calcd for $C_{63}H_{65}N_3OS_2$ 943.5). Anal. Calcd (%) for

$C_{63}H_{65}N_3OS_2$: C, 80.13; H, 6.94; N, 4.45; O, 1.69; S, 6.79. Found: C, 80.30; H, 6.81; N, 4.71.

*4.2.5. 4-(Bis-4-((E)-2-(9-octyl-9H-carbazol-2-yl)vinyl)phenyl)aminobenzaldehyde (**7**).* The synthetic method for compound **7** was similar to that of compound **5**. It was purified by column chromatography (silica gel, petroleum ether/CH_2Cl_2=1:1) to give yellow solid (65% in yield). Mp 76.0–78.0 °C. ^{1}H NMR (500 MHz, $CDCl_3$) δ=9.84 (s, 1H), 8.22 (d, *J*=5 Hz, 2H), 8.12 (d, *J*=7.5 Hz, 2H), 7.65–7.73 (m, 4H), 7.52 (t, *J*=9.0 Hz, 4H), 7.47 (t, *J*=7.5 Hz, 4H), 7.39–7.45 (m, 4H), 7.27–7.36 (m, 2H), 7.21–7.34 (m, 4H), 7.10–7.21(m, 4H) 4.29 (t, *J*=7.0 Hz, 4H), 1.19–1.54 (m, 24H), 0.86 (t, *J*=7.0 Hz, 6H) (Fig. S8). MS (MALDI-TOF): *m/z* 880.3 [M+H$^+$] (Fig. S9, calcd for $C_{63}H_{65}N_3O$ 879.5). Anal. Calcd (%) for $C_{63}H_{65}N_3O$: C, 85.97; H, 7.44; N, 4.77; O, 1.82. Found: C, 85.85; H, 7.66; N, 4.65.

*4.2.6. (E)-3-(4-(Bis-(4-(4-diphenylaminostyryl))-phenyl)amino)phenyl-2-cyanoacrylic acid (**TT**).* A mixture of compound **5** (0.10 g, 12.32 mmol), cyanoacetic acid (20.95 mg, 25 mmol), and ammonium acetate (20 mg) in glacial acetic acid (10 mL) was stirred at 120 °C for 12 h. After it was cooled to room temperature, the resulting precipitate was collected by filtration and washed with water. The crude product was purified by column chromatography (silica gel) using methanol/dichloromethane (v/v=1:10) as the eluent. 80 mg of red solid was obtained (74% in yield). Mp 174.0–176.0 °C. IR (KBr, cm^{-1}): 961, 1070, 1134, 1437, 1612, 2026, 2218, 2370, 2447, 2927, 3124, 3377 and 3441 cm^{-1}. ^{1}H NMR (500 MHz, DMSO-d_6) δ=8.12 (s, 1H), 7.93 (d, *J*=9.0 Hz, 2H), 7.60 (d, *J*=8.5 Hz, 4H), 7.51 (d, *J*=8.5 Hz, 4H), 7.32 (t, *J*=8.0 Hz, 8H), 7.16 (m, 8H), 7.05 (m, 12H), 7.00 (d, *J*=9.0 Hz, 2H), 6.96 (d, *J*=8.5 Hz, 4H) (Fig. S10). ^{13}C NMR (125 MHz, DMSO-d_6) δ=164.9, 154.1, 152.5, 147.6, 145.5, 145.0, 135.2, 133.8, 132.2, 130.9, 130.4, 128.5, 127.3, 127.0, 126.6, 125.0, 124.1, 123.9, 119.7, 119.0, 117.8, 99.0 (Fig. S11). MS (MALDI-TOF): *m/z* 878.7 [M$^+$] (Fig. S12, calcd for $C_{62}H_{46}N_4O_2$: 878.4). Anal. Calcd (%) for $C_{62}H_{46}N_4O_2$: C, 84.71; H, 5.27; N, 6.37; O, 3.64. Found: C, 84.50; H, 5.16; N, 6.67.

*4.2.7. (E)-3-(4-(Bis-(4-(E-2-(10-octyl-10H-phenothiazin-2-yl))vinyl)phenyl)amino)phenyl-2-cyanoacrylic acid (**TP**).* The synthetic procedure for **TP** was similar to that of **TT**. The crude product was purified by column chromatography (silica gel) using methanol/dichloromethane (v/v=1:10) as the eluent to give dark-red solid (64% in yield). Mp 164.0–166.0 °C. IR (KBr, cm^{-1}): 962, 1040, 1130, 1180, 1330, 1460, 1500, 1581, 2213, 2360, 2850, 2923, 3398, 3430 cm^{-1}; ^{1}H NMR (500 MHz, DMSO-d_6) δ=8.04 (s, 1H), 7.88 (d, *J*=8.50 Hz, 2H), 7.56 (d, *J*=8.0 Hz, 4H), 7.38 (d, *J*=7.5 Hz, 4H), 7.19 (t, *J*=7.5 Hz, 2H), 7.04–7.15 (m, 10H), 6.95 (m, 8H), 3.86 (m, 4H), 1.19–1.37 (m, 24H), 0.81 (t, *J*=7.0 Hz, 6H) (Fig. S13). ^{13}C NMR (125 MHz, DMSO-d_6) δ=164.9, 152.1, 151.4, 145.2, 144.9, 135.0, 133.1, 132.5, 128.5, 128.0, 127.8, 127.0, 126.9, 126.6, 125.4, 124.7, 124.0, 123.3, 120.9, 118.7, 116.7, 99.7, 67.8, 47.4, 32.0, 29.5, 29.4, 27.0, 26.9, 22.9, 14.8 (Fig. S14). MS (MALDI-TOF): *m/z* 1011.3 [M+H$^+$] (Fig. S15, Calcd for $C_{66}H_{66}N_4O_2S_2$: 1010.5). Anal. Calcd (%) for $C_{66}H_{66}N_4O_2S_2$: C, 78.38; H, 6.58; N, 5.54; O, 3.16; S, 6.34. Found: C, 78.29; H, 6.57; N, 5.43.

*4.2.8. (E)-3-(4-(Bis(4-((E)-2-(9-octyl-9H-carbazol-2-yl)vinyl)phenyl)amino)phenyl)-2-cyanoacrylic acid (**TC**).* The synthetic procedure for **TC** was similar to that of **TT**. The crude product was purified by column chromatography (silica gel) using methanol/dichloromethane (v/v=1:9) as the eluent to give a red solid (68% in yield). Mp 126.0–128.0 °C. IR (KBr, cm^{-1}): 962, 1070, 1133, 1268, 1382, 1440, 1612, 1710, 2030, 2220, 2440, 2925, 3135, 3378, 3441 cm^{-1}. ^{1}H NMR (500 MHz, DMSO-d_6) δ=8.38 (s, 1H), 8.18 (d, *J*=8.0 Hz, 2H), 7.94 (m, 4H), 7.73 (m, 2H), 7.65 (t, *J*=8.0 Hz, 4H), 7.59 (d, *J*=8.0 Hz, 4H), 7.41–7.47 (m, 4H), 7.38 (t, *J*=8.0 Hz, 2H), 7.26 (m, 4H), 7.17–7.21 (m, 2H), 6.94 (d, *J*=9.0 Hz, 2H), 4.38 (t, *J*=7.0 Hz, 4H), 1.04–1.27 (m, 24H), 0.81 (t, *J*=7.0 Hz, 6H) (Fig. S16). ^{13}C NMR (125 MHz, DMSO-d_6) δ=165.1, 153.3, 152.2, 146.1, 144.9, 141.3, 140.7, 135.7, 133.5, 130.9, 130.3, 130.0, 129.0, 128.3, 127.1, 126.9, 126.4, 125.5, 123.3, 123.0, 121.2, 119.8, 119.4, 118.2, 110.3, 100.4, 43.2, 32.0, 29.9, 29.6, 29.4, 27.3, 22.9, 14.8 (Fig. S17). MS (MALDI-TOF): m/z 947.2 [M+H$^+$] (Fig. S18, calcd for $C_{66}H_{66}N_4O_2$: 946.5). Anal. Calcd (%) for $C_{66}H_{66}N_4O_2$: C, 83.68; H, 7.02; N, 5.91; O, 3.38. Found: C, 83.59; H, 6.88; N, 6.07.

4.3. Theoretical calculation methods

The geometrical structures of the synthesized triphenylamine-based dyes were optimized by employing the density functional theory at the B3LYP/6-31 level with the Gaussian 03W program package.[22] Molecular orbitals were visualizable using Gaussview.

4.4. Preparation of dye-absorbed TiO_2 films

The dye-anchored TiO_2 film as a working electrode was prepared by following procedure. The area of the nanocrystalline-TiO_2 film coated on FTO glasses (2.2 mm thickness, 15 Ω/cm^2, Nippon Sheet Glass) was 0.24 cm^2 (0.55 cm of diameter). The film was dried in air at 100 °C for 15 min followed by another 15 min at 150 °C. Then, the film was calcined at 350 °C for 10 min. After that, the film was treated at 450 °C for 30 min under oxygen atmosphere. When the temperature decreased to 100 °C, the electrodes were immersed in a dry CH_2Cl_2 solution of the dye (0.5 mM) and kept at room temperature for 12 h.

A sandwich cell was prepared by using the dye-anchored TiO_2 film as a working electrode and Pt electrode as a counter one, which was assembled with a hot-melt-ionomer film of Surlyn polymer gasket. The electrodes were tightly held and heated at 120 °C for 25 s in seal machine (DHS-ES2) to seal the two electrodes. The aperture of the Surlyn frame was 2 mm larger than that of the area of TiO_2 film and its width was 1 mm. The hole in the counter electrode was sealed by a film of Surlyn. A drop of an electrolyte was put on the hole in the back of the counter electrode. It was introduced into the cell via vacuum backfilling. Finally, the hole was sealed using Surlyn film and a cover glass (0.13–0.17 mm thickness). The edge of the FTO outside of the cell was roughened with sandpaper. An electrolyte solution used was 0.6 M 1,2-dimethyl-3-methylimidazolium iodide, 0.1 M LiI, 0.05 M I_2, 0.5 M TBP, 4-*tert*-butylpyridine, and 0.05 mM GUSCN (guanidine thiocyanate) in dry acetonitrile.

4.5. Photovoltaic characterizations

Photoelectrochemical data were measured using a 150 W xenon light source that was focused to give 100 mW/cm^2 at the surface of the test cell. The spectral output of the lamp was matched with the aid of a Mega-9 AM 1.5 sunlight filter so as to reduce the mismatch between the simulated and the true solar spectrum. The applied potential and current were measured using a CHI 604B electrochemical working station. A similar data acquisition system was used to control the incident photon-to-current conversion efficiency (IPCE) measurement. Under full computer control, light from a 250 W halogen lamp was focused through a high throughput monochromator (Omni-λ150) onto the photovoltaic cell. The IPCE values were determined at 2 nm intervals.[7]

The solar energy-to-electricity conversion efficiency (η) of the DSSCs is calculated from the short-circuit photocurrent density (J_{sc}), the open-circuit photovoltage (V_{oc}), the fill factor of the cell (ff), and the intensity of the incident light (Pin).[7]

Acknowledgements

This work was supported by the Scientific Research Foundation for the Returned Overseas Chinese Scholars, State Education

Ministry; The National Natural Science Foundation of China (20874034 and 51073068); 973 Program (2009CB939701); Open Project of State Key Laboratory of Supramolecular Structure and Materials (SKLSSM201102).

Supplementary data

Supplementary data related to this article can be found in the online version, at doi:10.1016/j.tet.2012.02.077. These data include MOL files and InChIKeys of the most important compounds described in this article.

References and notes

1. O'Regan, B.; Grätzel, M. *Nature* **1991**, *353*, 737.
2. (a) Grätzel, M. *Acc. Chem. Res.* **2009**, *42*, 1788; (b) Grätzel, M. *Nature* **2001**, *414*, 338.
3. (a) Mishra, A.; Fischer, M. K. R.; Bäuerle, P. *Angew. Chem., Int. Ed.* **2009**, *48*, 2474; (b) Ooyama, Y.; Harima, Y. *Eur. J. Org. Chem.* **2009**, 2903; (c) Wang, X.; Tamiaki, H. *Energy Environ. Sci.* **2010**, *3*, 94.
4. (a) Zhang, G.; Bala, H.; Cheng, Y.; Shi, D.; Lv, X.; Yu, Q.; Wang, P. *Chem. Commun.* **2009**, 2198; (b) Liska, P.; Comte, P.; Péchy, P.; Grätzel, M. *Chem. Commun.* **2008**, 5194; (c) Choi, H.; Baik, C.; Kang, S. O.; Ko, J.; Kang, M. S.; Nazeeruddin, M. K.; Grätzel, M. *Angew. Chem., Int. Ed.* **2008**, *47*, 327; (d) Xu, M.; Wenger, S.; Bala, H.; Shi, D.; Li, R.; Zhou, T.; Zakeeruddin, S. M.; Grätzel, M.; Wang, P. *J. Phys. Chem. C* **2009**, *113*, 2966; (e) Kim, S.; Kim, D.; Choi, H.; Kang, M. S.; Song, K.; Kang, S. O.; Ko, J. *Chem. Commun.* **2008**, 4951; (f) Wang, Z. S.; Koumura, N.; Cui, Y.; Takahashi, M.; Sekiguchi, H.; Mori, A.; Kubo, T.; Furube, A.; Hara, K. *Chem. Mater.* **2008**, *20*, 3993; (g) Horiuchi, T.; Miura, H.; Sumioka, K.; Uchida, S. *J. Am. Chem. Soc.* **2004**, *126*, 12218; (h) Kim, S.; Lee, J. K.; Kang, S. O.; Ko, J.; Yum, J. H.; Fantacci, S.; De Angelis, F.; Censo, D. D.; Nazeeruddin, M. K.; Grätzel, M. *J. Am. Chem. Soc.* **2006**, *128*, 16701; (i) Bessho, T.; Zakeeruddin, S. M.; Yeh, C.-Y.; Diau, E. W.; Grätzel, M. *Angew. Chem., Int. Ed.* **2010**, *49*, 6646; (j) Yum, J.; Hagberg, D. P.; Moon, S.; karlsson, K. M.; Marinado, T.; Sun, L.; Hagfeldt, A.; Nazeeruddin, M. K.; Grätzel, M. *Angew. Chem., Int. Ed.* **2009**, *48*, 1576; (k) Kim, S. H.; Choi, H. B.; Baik, C.; Song, K. Y.; Kanga, S. O.; Ko, J. *Tetrahedron* **2007**, *63*, 11436; (l) Matsui, M.; Asamura, Y.; Kubota, Y.; Funabiki, K.; Jin, J.; Yoshida, T.; Miura, H. *Tetrahedron* **2010**, *66*, 7405; (m) Velusamy, M.; Thomas, K. R. J.; Lin, J. T.; Hsu, Y. C.; Ho, K. C. *Org. Lett.* **2005**, *7*, 1899; (n) Thomas, K. R. J.; Hsu, Y. C.; Lin, J. T.; Lee, K. M.; Ho, K. C.; Lai, C. H.; Cheng, Y. M.; Chou, P. T. *Chem. Mater.* **2008**, *20*, 1830; (o) Yang, C. H.; Liao, S. H.; Sun, Y. K.; Chuang, Y. Y.; Wang, T. L.; Shieh, Y. T.; Lin, W. C. *J. Phys. Chem. C* **2010**, *114*, 21786; (p) Teng, C.; Yang, X. C.; Yang, C.; Tian, H. N.; Li, S. F.; Wang, X. N.; Hagfeldt, A.; Sun, L. C. *J. Phys. Chem. C* **2010**, *114*, 11305; (q) Tiana, H.; Yanga, X.; Chena, R.; Pana, Y.; Li, L.; Hagfeldt, A.; Sun, L. C. *Chem. Commun.* **2007**, 3741; (r) Teng, C.; Yang, X. C.; Yuan, C. Z.; Li, C. Y.; Chen, R. K.; Tian, H. N.; Li, S. F.; Hagfeldt, A.; Sun, L. C. *Org. Lett.* **2009**, *11*, 5542; (s) Hara, K.; Sayama, K.; Ohga, Y.; Shinpo, A.; Suga, S.; Arakawa, H. *Chem. Commun.* **2001**, 569; (t) Ehret, A.; Stuhl, L.; Spitler, M. T. *J. Phys. Chem. B* **2001**, *105*, 9960; (u) Yao, Q. H.; Meng, F. S.; Li, F. Y.; Tian, H.; Huang, C. H. *J. Mater. Chem.* **2003**, *13*, 1048; (v) Sayama, K.; Tsukagoshi, S.; Mori, T.; Hara, K.; Ohga, Y.; Shinpou, A.; Abe, Y.; Suga, S.; Arakawa, H. *Sol. Energy Mater. Sol. Cells* **2003**, *80*, 47; (w) Ferrere, S.; Gregg, B. A. *New J. Chem.* **2002**, *26*, 1155.
5. (a) Liu, D.; Fessenden, R. W.; Hug, G. L.; Kamat, P. V. *J. Phys. Chem. B* **1997**, *101*, 2583; (b) Hara, K.; Wang, Z.; Sato, T.; Furube, A.; Katoh, R.; Sugihara, H.; Dan-oh, Y.; Kasada, C.; Shinpo, A.; Suga, S. *J. Phys. Chem. B* **2005**, *109*, 15476; (c) Ning, Z.; Zhang, Q.; Wu, W.; Pei, H.; Liu, B.; Tian, H. *J. Org. Chem.* **2008**, *73*, 3791; (d) Ning, Z.; Zhang, Q.; Pei, H.; Luan, J.; Lu, C.; Cui, Y.; Tian, H. *J. Phys. Chem. C* **2009**, *113*, 10307.
6. Zhou, H. P.; Xue, P. C.; Zhang, Y.; Zhao, X.; Jia, J. H.; Zhang, X. F.; Liu, X. L.; Lu, R. *Tetrahedron* **2011**, *67*, 8477.
7. Xu, W.; Peng, B.; Chen, J.; Liang, M.; Cai, F. *J. Phys. Chem. C* **2008**, *112*, 874.
8. Wu, W. J.; Yang, J. B.; Hua, J. L.; Tang, J.; Zhang, L.; Long, Y. T.; Tian, H. *J. Mater. Chem.* **2010**, *3*, 1772.
9. (a) Hagberg, D. P.; Yum, J.-H.; Lee, H.; De Angelis, F.; Marinado, T.; Karlsson, K. M.; Humphry-Baker, R.; Sun, L.; Hagfeldt, A.; Grätzel, M.; Nazeeruddin, M. K. *J. Am. Chem. Soc.* **2008**, *130*, 6259; (b) Fischer, M. K. R.; Wenger, S.; Wang, M.; Mishra, A.; Zakeeruddin, S. M.; Grätzel, M.; Bäuerle, P. *Chem. Mater.* **2010**, *22*, 1836; (c) Lee, C.; Zhang, Y.; Romayanantakit, A.; Galoppini, E. *Tetrahedron* **2010**, *66*, 3897; (d) Zhang, L.; Liu, Y. K.; Wang, Z. Y.; Liang, M.; Sun, Z.; Xue, S. *Tetrahedron* **2010**, *66*, 3318.
10. Li, K. P.; Qu, J. L.; Xu, B.; Zhou, Y. H.; Liu, L. J.; Peng, P.; Tian, W. J. *New J. Chem.* **2009**, *33*, 2120.
11. Qiu, X. P.; Lu, R.; Zhou, H. P.; Zhang, X. F.; Xu, T. H.; Liu, X. L.; Zhao, Y. Y. *Tetrahedron* **2007**, *48*, 7582.
12. Yang, X. C.; Lu, R.; Zhou, H. P.; Xue, P. C.; Wang, F. Y.; Chen, P.; Zhao, Y. Y. *J. Colloid Interface Sci.* **2009**, *2*, 527.
13. (a) Li, B. S.; Li, J.; Fu, Y. Q.; Bo, Z. S. *J. Am. Chem. Soc.* **2004**, *126*, 3430; (b) Li, B.; Xu, X.; Sun, M.; Fu, Y.; Yu, G.; Liu, Y.; Bo, Z. S. *Macromolecules* **2006**, *39*, 456.
14. Tang, J.; Hua, J. L.; Wu, W. J.; Li, J.; Jin, Z. G.; Long, Y. T.; Tian, H. *Energy Environ. Sci.* **2010**, *3*, 1736.
15. Chen, H.; Huang, H.; Huang, X.; Clifford, J. N.; Forneli, A.; Palomares, E.; Zheng, X.; Zheng, L.; Wang, X.; Shen, P.; Zhao, B.; Tan, S. *J. Phys. Chem. C* **2010**, *114*, 3280.
16. Hagberg, D. P.; Marinado, T.; Karlsson, K. M.; Nonomura, K.; Qin, P.; Boschloo, G.; Brinck, T.; Hagfeldt, A.; Sun, L. C. *J. Org. Chem.* **2007**, *72*, 9550.
17. Choi, H.; Lee, J. K.; Song, K.; Kang, S. O.; Ko, J. *Tetrahedron* **2007**, *63*, 3115.
18. Huang, S. Y.; Schlichthorl, G.; Nozik, A. J.; Grätzel, M.; Frank, A. J. *J. Phys. Chem. B* **1997**, *101*, 2576.
19. Marinado, T.; Nonomura, K.; Nissfolk, J.; Karlsson, M. K.; Hagberg, D. P.; Sun, L.; Mori, S.; Hagfeldt, A. *Langmuir* **2010**, *26*, 2592.
20. Liang, M.; Xu, W.; Cai, F. S.; Chen, P. Q.; Peng, B.; Chen, J.; Li, Z. M. *J. Phys. Chem. C* **2007**, *111*, 4465.
21. Liang, Y. L.; Peng, B.; Liang, J.; Tao, Z. L.; Chen, J. *Org. Lett.* **2010**, *12*, 1204.
22. Frisch, M. J.; Trucks, G. W.; Schlegel, H. B.; Scuseria, G. E.; Robb, M. A.; Cheeseman, J. R. J. A.; Montgomery, J.; Vreven, T.; Kudin, K. N.; Burant, J. C.; Millam, J. M.; Iyengar, S. S.; Tomasi, J.; Barone, V.; Mennucci, B.; Cossi, M.; Scalmani, G.; Rega, N.; Petersson, G. A.; Nakatsuji, H.; Hada, M.; Ehara, M.; Toyota, K.; Fukuda, R.; Hasegawa, J.; Ishida, M.; Nakajima, T.; Honda, Y.; Kitao, O.; Nakai, H.; Klene, M.; Li, X.; Knox, J. E.; Hratchian, H. P.; Cross, J. B.; Adamo, C.; Jaramillo, J.; Gomperts, R.; Stratmann, R. E.; Yazyev, O.; Austin, A. J.; Cammi, R.; Pomelli, C.; Ochterski, J.; Ayala, P. Y.; Morokuma, K.; Voth, G.; Salvador, P.; Dannenberg, J. J.; Zakrzewski, V. G.; Dapprich, S.; Daniels, A. D.; Strain, M. C.; Farkas, O.; Malick, D. K.; Rabuck, A. D.; Raghavachari, K.; Foresman, J. B.; Ortiz, J. V.; Cui, Q.; Baboul, A. G.; Clifford, S.; Cioslowski, J.; Stefanov, B. B.; Liu, G.; Liashenko, A.; Piskorz, P.; Komaromi, I.; Martin, R. L.; Fox, D. J.; Keith, T.; Al-Laham, M. A.; Peng, C. Y.; Nanayakkara, A.; Challacombe, M.; Gill, P. M. W.; Johnson, B.; Chen, W.; Wong, M. W.; Gonzalez, C.; Pople, J. A.; Gaussian 03, Revision C. 02. Wallingford, CT: Gaussian, 2004.